From Low- to High-Dimensional Dynamics in a Microscopic Fluid Flow

T. Peacock,* D. J. Binks, and T. Mullin

Department of Physics and Astronomy, Manchester University, Manchester M13 9PL, United Kingdom

(Received 1 July 1998)

The results of an experimental study of flow in a small aspect ratio liquid crystal cell are presented where the dimensions of the device are on the same scale as the width of a human hair. This system is found to display wide ranging dynamical behavior, from simple oscillations to seemingly homogeneous turbulence. Through a systematic study of the low-dimensional behavior we uncover an organizing center for the dynamics. [S0031-9007(99)08414-8]

PACS numbers: 47.20.Ky, 47.65.+a, 61.30.Gd

The nature of turbulence and the mechanisms by which it can arise have been investigated in many different experimental geometries. In classical systems displaying a hydrodynamic instability, such as Rayleigh-Bénard convection or Taylor-Couette flow, ideas based upon dynamical systems theory have provided insight into the origins of complicated fluid motion [1,2]. This insight has yet to have a significant impact on our understanding of the physics of turbulence, however. Indeed the Taylor-Couette system, perhaps the most richly explored small aspect ratio experiment [3], does not become fully turbulent even at high Reynolds numbers as cellular structure remains in the flow.

Another instability problem which has in recent years become the focus of much attention is the instability to cellular convection in an electrically driven nematic liquid crystal, commonly referred to as electroconvection [4]. A nematic is a complex fluid composed of rod or disklike molecules which possess orientational but not positional order. It exhibits complicated flow properties due to a coupling between translational and orientational motions of the molecules. If an electric field is applied to an appropriately aligned nematic confined between parallel glass plates cellular convection can occur above a critical field strength. Associated with the convection is a distortion of the original alignment which is manifest as a spatially varying refractive index. This enables flow to be observed directly as an intensity pattern formed by the focusing and defocusing of transmitted light.

Experimental investigations of electroconvection have typically been concerned with large aspect ratio systems containing many convection cells. Under these conditions it is assumed that one can describe the onset of cellular convection and subsequent transitions using general arguments about pattern formation in nonequilibrium systems [4,5]. In these circumstances it is difficult to investigate low-dimensional dynamics, however, since the multiplicity of flows can be immeasurably large [6]. The potential for such behavior is thus obscured by inevitable fluctuations that cause the system to jump between the many coexisting states. However, small aspect ratio electroconvection experiments can exhibit low-dimensional behavior [7]. Despite this observation, relatively little work has been done on the origin of this complex time dependency.

In this Letter we present experimental results which are in accord with ideas from simple low-dimensional models. Furthermore, we give evidence for strongly turbulent fluid motion. These observations, in combination with issues raised by the extremely small scale of the system, offer possible insight into the links between the nature of turbulence in liquid crystals and low-dimensional fluid motion.

The liquid crystal cell comprised a $46 \pm 1.0\ \mu$m thick layer of nematic liquid crystal BDH-17886 sandwiched between two optically flat glass plates. An indium-tin oxide line electrode of thickness $\sim 185\ \mu$m was etched onto the inner surface of each plate and the arrangement was such that, when viewed from above, the lines overlapped at right angles. This created an active region of aspect ratio 4:4:1 to which an electric field could be applied. The largest dimension of the active area was equivalent to only 10^5 molecular lengths and comparable to the width of a human hair, as illustrated in Fig. 1(a). On such a small scale inherent microscopic fluctuations are known to cause large variation in continuum quantities such as the director (the unit vector field describing the macroscopic average of molecular orientation) [8]. Alignment of the material, which was parallel to the lower electrode, was obtained using a rubbed layer of polyvinyl alcohol spin coated on top of the electrodes. The cell was mounted on a microscope translation stage and maintained at a constant temperature of $32.0 \pm 0.02\,^{\circ}$C. Applied ac voltages were of the order of 10 $V_{\rm rms}$ and had a frequency of the order of 600 Hz. These parameters had a long term stability of better than 0.5%. Light transmitted through the cell was imaged using a CCD camera and analyzed using a computer imaging system.

An image of eight-cell flow in the liquid crystal cell is presented in Fig. 1(b). Within a given parameter range this flow was primary [9,10]; i.e., it smoothly evolved from the undisturbed nematic as the voltage V was continuously increased or the frequency F was continuously reduced. In neighboring regions of parameter space the primary flow comprised six or ten convection cells.

 0031-9007/99/82(7)/1446(4)$15.00

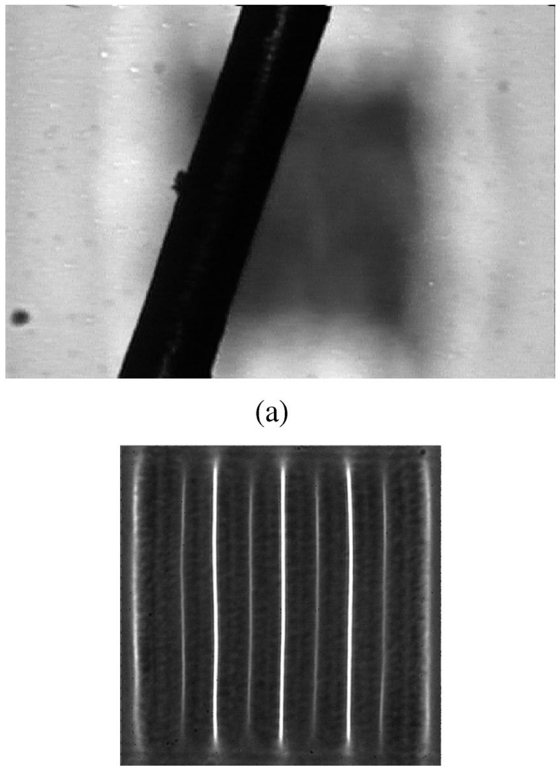

FIG. 1. (a) Image of the cell through a microscope, with a human hair placed directly above the cell. The out of focus square shape beneath is caused by the fluid motion inside the active region. (b) The eight-cell primary flow. Bright intensity lines indicate upward convective flow and fainter lines indicate downward motion. Thus, in between two bright intensity lines there is a pair of counterrotating convection cells. Only the active region is shown.

By systematically varying V and F a two-dimensional experimental bifurcation set could be determined for the eight-cell flow. A nondimensional scheme [11] was used where a voltage reference value V_{ref} was defined to be the lowest voltage at which the eight-cell flow remained primary. In a like manner, the frequency reference value F_{ref} was defined to be the highest frequency at which a six-cell flow was primary. The nondimensionalized variables were therefore $v = V/V_{\mathrm{ref}}$ and $f = F/F_{\mathrm{ref}}$. Both V_{ref} and F_{ref} were measured regularly during experimental runs and the location of a bifurcation point in (v, f) parameter space could typically be determined with an accuracy of 0.1%.

The steady eight-cell flow was found to undergo two different types of transitions as f was smoothly decreased. For $v > 1.037$ a reversible transition to time-dependent behavior occurred. The resulting singly periodic flow was characterized by a "breaking" and "joining" of the convection cells with a period of the order of 35 sec. This flow is qualitatively similar to that reported by Tsuchiya *et al.* [7]. Adopting the method of Yang *et al.* [12], the amplitude of oscillation was quantified by measuring the displacement of a selected maximum in the intensity pattern. An alternative measure concerned with intensity variation at a point in the intensity pattern [13] could not be used as it proved to be nonlinear in this case due to the large amplitude of the director distortion. The amplitude and frequency of the oscillations are plotted as a function of f in Fig. 2 for $v = 1.331$. A square root curve has been fitted to the amplitude measurements and a linear fit has been applied to the frequency measurements. The results fit well to these curves, which correspond to leading terms in the truncated normal form for a supercritical Hopf bifurcation. In Fig. 3, which is an experimental bifurcation set for the system, the line OA has been drawn through a locus of experimentally determined Hopf bifurcation points. As this line was crossed from above the steady eight-cell flow became unstable to time-dependent behavior. It was found that the period of oscillation at onset increased monotonically towards the point O.

For $v < 1.037$ the eight-cell flow disappeared at a critical value of the control parameter and the system evolved onto a symmetry broken steady eight-cell flow state. The transition was irreversible so that the eight-cell flow could not be regained by increasing f back through the critical value. Such behavior is consistent with a saddle-node bifurcation. Here the stable solution branch corresponds to the steady eight-cell flow, and the unstable

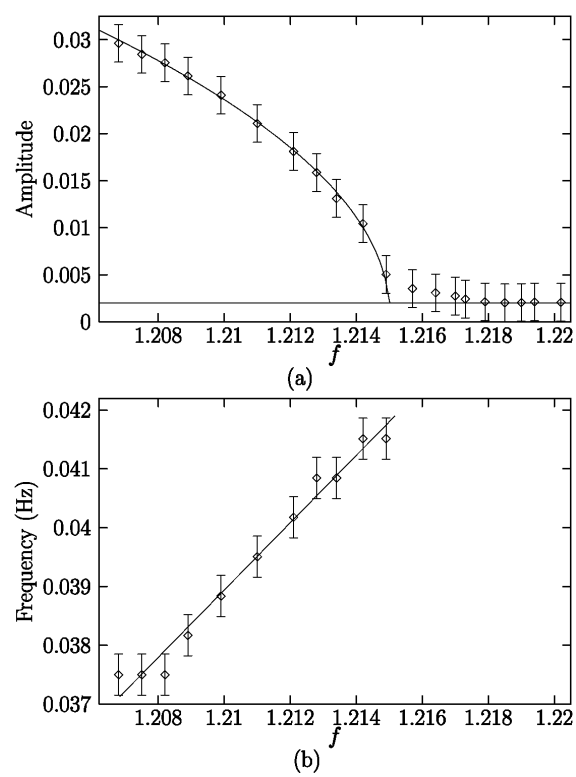

FIG. 2. Hopf bifurcation results for the eight-cell flow for $v = 1.331$. (a) Amplitude measurements. (b) Frequency measurements.

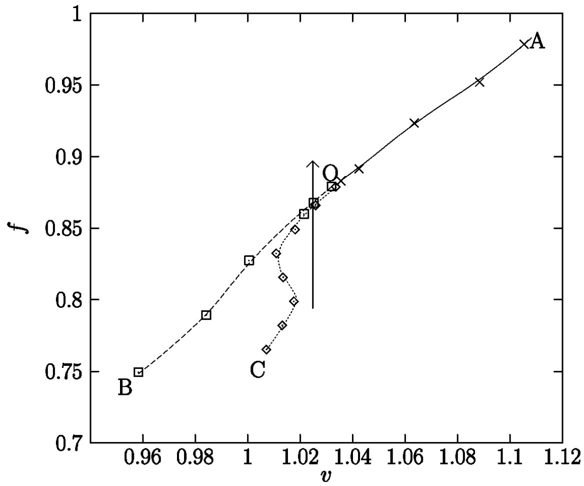

FIG. 3. The experimentally determined bifurcation set for the eight-cell flow. OA is a line of Hopf bifurcations; OB is a line of saddle-node bifurcations; OC is a line of homoclinic bifurcations. The arrow indicates the parameter path followed when obtaining the results presented in Fig. 4.

solution branch is a steady cellular flow which cannot be realized experimentally. In Fig. 3 the line OB has been drawn through a locus of experimentally determined saddle-node bifurcation points.

The point O in Fig. 3, at which the saddle-node and Hopf bifurcations merge, is a codimension-2 point of bifurcation since it requires judicious variation of both v and f in order to be encountered. The region of parameter space surrounding such a multiple bifurcation point is known to provide a regime in which insight gained from simple theoretical models can be used to interpret experimental observations [6]. A model for a saddle-node/Hopf interaction was derived simultaneously, and independently, by both Takens and Bogdanov [14,15]. In addition to lines of Hopf and saddle-node bifurcations, the model contains a line of homoclinic bifurcations originating from the codimension-2 point.

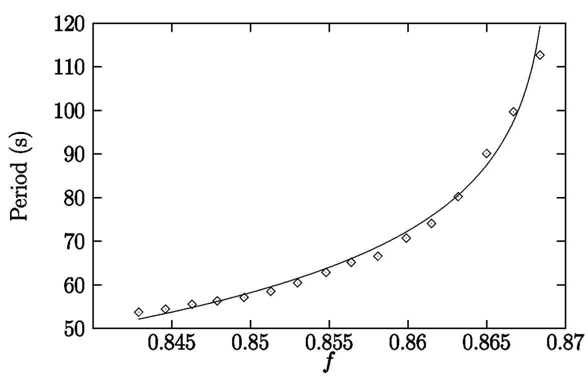

FIG. 4. Measurements of period of the eight-cell time-dependent flow for $v = 1.024$. The arrow in Fig. 3 indicates the parameter path followed when obtaining these results.

Through a systematic variation of v and f an additional line of bifurcations, labeled OC in Fig. 3, was found to originate from the codimension-2 point. As this line of critical points was approached from the right-hand side and/or below the period of the time-dependent eight-cell flow increased monotonically, as illustrated by the measurements presented in Fig. 4. The arrow in Fig. 3 indicates the parameter path followed to obtain these measurements. A logarithmic function, typical of a homoclinic connection [16], has been fitted to the results. As the line OC was crossed the flow collapsed irreversibly onto the symmetry broken eight-cell steady flow obtained by traversing the line OB from above. The line OC is the locus of points of closest approach to an infinite period in our system and so is our estimate of the line of homoclinic bifurcations emanating from the Takens-Bogdanov point O [17].

Detailed investigations revealed that there were no other states involved in the reported interaction. As such, we conjecture that the model of Takens and Bogdanov is the simplest that can account for the observed local and global behavior. However, establishing a 1:1 correspondence between the model bifurcation set, in which the lines of Hopf and homoclinic bifurcations are tangent at the codimension-2 point, and the experimental set presented in Fig. 3, where they approach O from opposite sides, is problematical. The results imply a nontrivial relationship between physical and abstract parameters, so that the experimental bifurcation set arises as a complicated projection from abstract to physical parameter space. Sufficiently close to a codimension-2 point one would expect linear terms to dominate the relation between abstract and physical parameters, but it was not possible to resolve such a regime in the experiment. It should also be noted that within the context of the model system, OB corresponds to one-half of a line of saddle-node bifurcations. The other half, an unstable solution branch also orginating from O, must exist between OB and OC but could not be determined experimentally.

As the forcing was increased away from the codimension-2 point, for example, by smoothly increasing the voltage, the pattern dynamics first became more temporally disordered. Within this regime the behavior of cellular flows could be related to low-dimensional models [21], such as those proposed by Shil'nikov [22] and Arnéodo *et al.* [23]. Increasing v further still, additional spatial modes were excited and weak turbulence developed [24]. Commonly referred to as spatiotemporal chaos [25], this state was characterized by the existence of cellular structures that no longer retained any consistent form. A smooth transition to seemingly turbulent flow then ensued as v was raised to approximately twice the value at which steady flow was observed. An image of the turbulent motion is presented in Fig. 5, in which it can be seen that fluid motion extended beyond the boundaries of the active region imposed by the electrode

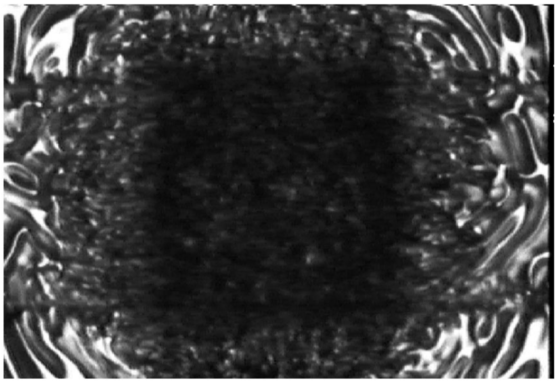

FIG. 5. Turbulent flow in the liquid crystal cell. The central dark square region is the volume in which the turbulent flow is excited by the applied field.

configuration. This regime is commonly referred to as the dynamic scattering mode [26] and is known to contain singularities on distances comparable to some 10 to 100 molecular lengths [8]. Under such conditions one might question the validity of a continuum approximation for modeling the flow field.

A striking characteristic of the turbulent flow in Fig. 5 is that it is featureless, in contrast to the behavior found in other cellular flow problems. Indeed there is no evidence of the existence of coherent structures such as those that can be found in many classical turbulent flows. To all intents and purposes the nematic ordering is destroyed and the qualitative appearance is of a homogenous state. The stress applied to the system, by virtue of the voltage, is of the same order of magnitude as that required to generate the time-dependent motion. This is in stark contrast to the 3 orders of magnitude separation observed in Rayleigh number between oscillations and hard classical turbulence in a small aspect ratio Rayleigh-Bénard experiment [27].

In conclusion, we have observed low-dimensional dynamics and the appearance of highly disordered motion in a complex fluid system on a microscopic scale. That both of these states existed at comparable levels of forcing in a small aspect ratio system is unusual and intriguing.

This work was supported by the EPSRC and SHARP Laboratories of Europe Ltd.

*Currently at the Department of Computer Science, University of Colorado, Boulder, CO 80309.

[1] See, for instance, H. L. Swinney and J. P. Gollub, *Hydrodynamic Instabilities and the Transition to Turbulence* (Springer-Verlag, Berlin, 1981).
[2] A. Libchaber and J. Maurer, J. Phys. (Paris), Colloq. **41**, C3-51 (1980).
[3] J. von Stamm, Th. Buzug, and G. Pfister, Phys. Lett. A **194**, 173 (1994); Th. Buzug, J. von Stamm, and G. Pfister, Phys. Rev. E **47**, 1054 (1993).
[4] L. Kramer and W. Pesch, in *Pattern Formation in Liquid Crystals* (Springer-Verlag, New York, 1996).
[5] M. Dennin, D. S. Cannell, and G. Ahlers, Phys. Rev. E **57**, 638 (1998).
[6] T. Mullin, *The Nature of Chaos* (Oxford University Press, New York, 1993).
[7] Y. Tsuchiya, S. Horie, and H. Itakura, J. Phys. Soc. Jpn. **57**, 669 (1988).
[8] P. G. deGennes and J. Prost, *The Physics of Liquid Crystals* (Oxford University Press, New York, 1995).
[9] T. B. Benjamin, Proc. R. Soc. London A **359**, 1 (1978).
[10] D. J. Binks and T. Mullin, Proc. R. Soc. London A **453**, 2109 (1997).
[11] S. Kai and K. Hirakawa, Prog. Theor. Phys. Suppl. **64**, 212 (1978).
[12] C-Y. Yang *et al.*, J. Phys. Soc. Jpn. **55**, 703 (1986).
[13] I. Rehberg *et al.*, Phys. Rev. Lett. **67**, 596 (1991).
[14] F. Takens, Publ. Math. IHES **43**, 47 (1974).
[15] R. I. Bogdanov, Funct. Anal. Appl. **9**, 144 (1975).
[16] P. Gaspard, J. Phys. Chem. **94**, 1 (1990).
[17] Other types of codimension-2 points have previously been reported in experiments of Rayleigh-Bénard convection [18] and Taylor-Couette flow [19,20].
[18] I. Rehberg and G. Ahlers, Phys. Rev. Lett. **55**, 500 (1985).
[19] T. Mullin, K. A. Cliffe, and G. Pfister, Phys. Rev. Lett. **58**, 2212 (1987).
[20] T. Mullin, S. Tavener, and K. A. Cliffe, Europhys. Lett. **8**, 251 (1989).
[21] T. Peacock and T. Mullin (to be published).
[22] L. P. Shil'nikov, Sov. Math. Dokl. **6**, 163 (1965).
[23] A. Arnéodo, P. Coullet, and C. Tresser, Phys. Lett. **81A**, 197 (1981).
[24] P. Manneville, *Dissipative Structures and Weak Turbulence* (Academic Press, Boston, 1990).
[25] M. C. Cross and P. C. Hohenberg, Rev. Mod. Phys. **65**, 851 (1993).
[26] A. Joets and R. Ribotta, J. Phys. (Paris) **47**, 595 (1986).
[27] A. Libchaber, Proc. R. Soc. London A **413**, 63 (1987).